Research Square

Preprints are preliminary reports that have not undergone peer review.
They should not be considered conclusive, used to inform clinical practice,
or referenced by the media as validated information.

Growth of Pd decorated SiCN nanoballs for hydrogen gas sensing applications in extreme environment

Narendra Singh
Munshi Singh College Motihari, B. R. Ambedkar Bihar University Muzaffarpur
Hans Kumar Singh
T.P.S College, Patliputra, University
Mamta Rawat
B. R. Ambedkar Bihar University Muzaffarpur
Mukesh Kumar
SB&AS, Shree Guru Gobind Singh Tricentenary University
Vinay Kumar
COBS&H, CCS Haryana Agricultural University
Arvind Kumar
arvindkumar@rkclnmu.ac.in

R.K. College, Lalit Narayan Mithila University

Research Article

Keywords: Hydrogen, Sensor, Nanoballs, Silicon Carbide Nitride, Porous silicon

Posted Date: May 18th, 2026

DOI: https://doi.org/10.21203/rs.3.rs-9525978/v1

License: This work is licensed under a Creative Commons Attribution 4.0 International License.
Read Full License

Additional Declarations: No competing interests reported.

Version of Record: A version of this preprint was published at Applied Physics A on August 5th, 2026.
See the published version at https://doi.org/10.1007/s00339-026-10039-w.

Abstract

In this work, the H_2 gas sensing characteristics can be improved significantly by enhancing the effective exposure surface area and the surface reactivity of silicon carbide nitride (SiCN) nanoball sensor. The porous silicon (P-Si) substrates were synthesized by the electrochemical anodization method at room temperature (RT). Here, we have fabricated SiCN nanoballs (NBs) sensor on porous Si substrates via RF magnetron sputtering. The as prepared SiCN nanoballs were uniformly decorated with dispersed Pd nanoparticles on the sensor surface, resulting in a remarkable improvement of the surface reactivity. The H_2 gas sensing performance along with the sensing mechanism of the developed Pd/SiCN NBs sensor were discussed in detail under low detection level (2-200 ppm) at high working temperature regime (40–450 °C). In addition, the main measurements such as selectivity, stability, and cyclability were performed for better device applications. Therefore, porous silicon (P-Si) substrates uncover a new scientific approach for fabrication of high performance H_2 sensor in punitive environment.

1. Introduction

In recent years, widespread researches have been devoted to study numerous innovative methods that how to connect alternative prime energy sources causing negligible pollution and global warming in the wake of ultimate reduction of fossil fuels. H_2 has become an encouraging clean energy source under consideration to replace traditional fossil fuel due to its abundance, easy synthesis and eco-friendly nature [1–4]. However, when concentration of H_2 surpasses beyond 4% by volume, then at the same time it becomes an explosive in air. Since, hydrogen is odorless, tasteless, and colorless so it is very difficult to identified by human senses [5, 6]. In addition, H_2 gas causes corrosion of steel and other metals by penetrating inside these metals at elevated temperatures, which deteriorates these metals internally [7]. Nowadays, hydrogen sensors are in quite demand as essential component of numerous industries such as petroleum, chemical, and rubber industries which require storage tank and refining process. Moreover, hydrogen is very beneficial in food processing, rocket propulsion, semiconductor industries, internal combustion engine, fuel cell and nuclear reactors. Hence, systematic monitoring of H_2 gas molecules is essential requirement for safety of human being in futuristic and existing industries.

In last few years, several nano scale materials with their desired structures have been studied as H_2 gas sensor. Among various nanostructures, few of them are capable to do their work suitably in harsh environmental conditions. Among several gas sensors, chemiresistive based gas sensors are the most promising sensing devices that depend on change in electrical resistance with impressive diffusion and adsorption of analyzing gas during sensing [8–10]. Basically, these gas sensors are most advantageous due to their unique characteristics of low cost, eco-friendly, high sensitivity, and highly stable for a long-term [11–13]. The proposed sensing element is very useful for high temperature applications in space science and technology [14, 15]. In addition, SiCN can sustain harsh conditions such as high temperature radiation. It has excellent mechanical strength, durability, high corrosion and wear resistance. Usually wide band gap semiconductors such as SiC and GaN etc. are considered to withstanding high

temperature and corrosive environment [16–19]. In most of previous studies, silicon carbide (SiC) has fascinated the greater interest as a capable H_2 gas sensor due to its feasibility to operate at high temperature [20–23].

To further improve the performance of SiC-based H_2 gas sensor at higher operating temperatures, a strategic wide band gap material as compared to SiC is required to be employed [24]. It can be seen that the silicon nitride (Si_3N_4) has band gap of 5 eV and other properties are also slightly collaborated with SiC [24]. Silicon carbide exhibits the band gap value from 2.4 to 3.2 eV. However, band gap of SiCN thin films can be varies from 2.4 to 5 eV (it may depict the presence of both Si_3N_4 and SiC phases) [24]. Thus, it is expected that SiCN thin films exhibit broader band gap than SiC thin film. It may reveal the enhanced H_2 gas sensing properties at higher operating temperatures in harsh environmental conditions. Moreover, from the viewpoint of sensing properties, porous nanostructures are promising candidate materials due to their unique properties such as large specific surface area available for analyte gas molecules [25–28].

In this paper, for the first time SiCN thin films have been fabricated on electrochemically etched porous Si substrate by radio-frequency (RF) reactive magnetron sputtering by using a 5 cm diameter and 5 mm thick SiC target at RT. Herein, N_2 gas was used as a reactive gas and mixed with argon using mass flow controller (MFC). The prepared SiCN thin films as sensing layer were catalytically activated by depositing an ultra-thin (~ 5 nm) layer of Pd using DC sputtering method. Detailed microstructure, surface morphology along with H_2 gas sensing features of these films were studied under low detection limit (2-200 ppm) at elevated temperature (400 °C). In, this work, the outcomes are recognized as the developed SiCN thin film may be a promising electrode material to detect lower level (ppm) of hydrogen gas in harsh environmental conditions.

2. Experimental section

2.1 Materials and chemicals used

In, this work, highly pure (99.9%) gas cylinders of Nitrogen (N_2), Argon (Ar), hydrogen (H_2) and dry air were also procured from Sigma gases, India. Highly pure (99.99%) silicon carbide (SiC) sputtering target of 5 cm diameter and 5 mm thick was obtained from ACI Alloys Inc. USA. Chemicals such as isopropyl alcohol, acetone, ethanol (C_2H_5OH), hydrofluoric acid (HF) and nitric acid (HNO_3) were purchased from Merck, India. The R_g was measured in H_2, CO and H_2S gases balanced with dry air. All the gases were purchased from Sigma gases and services, New Delhi, India. For making electronic connections the silver (Ag) paste was also procured from SPI supplies USA. Single crystalline, (100) oriented, p-type Si substrates with an electrical resistivity 0.04–0.06 Ω-cm and thickness of 0.5 mm were purchased from Excel instruments, India.

2.2 Fabrication of sensor element

Firstly, highly doped p-type silicon wafers with orientation of (100) were cut into 1x1 cm^2 and rinsed properly in acetone and isopropyl alcohol by ultra-sonication for 15 minutes. Thereafter, these ultra-sonicated silicon wafers were cleaned in de-ionized (DI) water and dried carefully under argon flow. Pores on the cleaned silicon substrates were produced using custom designed electrochemical anodization setup (Fig. 1). In Fig. 1, (-ve) means platinum electrode which acts as a cathode and (+ ve) means copper plate that acts as an anode during anodization process. Characteristic properties of as-grown silicon pores are function of process parameters and solution used. Porous silicon (PSi) is synthesized by a controlled chemical reaction at the surface of silicon in aqueous ethanol (C_2H_5OH) and hydrogen fluoride (HF) solution. In this electrochemical etching process, H ions and molecules played a significant role as an intermediate products in the presence of electric field. It is observed that holes are the requisites to initiate the dissolution of Si to form H_2SiF_6 which is soluble in ethanol. Thereafter, the anodic current drives the primary dissolution reaction and dissolution of a silicon atom leads to the generation of 2 hydrogen atoms and 2 electrons [29]. The general anodic reactions occurring during the formation of pores are shown below:

$$\mathrm{Si} + 6\mathrm{HF} \rightarrow \ \mathrm{H_2SiF_6} + 2\mathrm{H^+} + \mathrm{H_2} + 2\mathrm{e^-} \qquad (1)$$

$$\mathrm{H_2SiF_6} \rightarrow \ \mathrm{SiF_6^{2-}} + 2\mathrm{H^+} \qquad (2)$$

Before starting the etching process, silicon substrate was gently tailored over the copper plate which acts as anode. A solution of hydrofluoric acid (HF) and ethanol solution in a 1:5 volumetric ratio is poured in the anodization chamber made up of teflon (Fig. 1). Moreover, a platinum (Pt) mesh as a cathode was also used in the solution to act as a counter electrode (Fig. 1). Thereafter, apply a current density of 40 mA/cm^2 using a direct current power supply constantly, for a time of 60 minutes at atmospheric temperature (optimized parameters). After completing this reaction, the as prepared porous substrates were carried out from the anodization chamber and cleaned in de-ionized (DI) water.

In this work, the SiCN thin films were synthesized on porous Si substrates by RF sputtering technique at RT. In sputtering, nitrogen gas was used as a reactive gas and argon gas was used to initiate the plasma inside the sputtering chamber. The rotary and turbo molecular pump (TMP) were used to achieve the high quality vacuum inside the sputtering chamber. Prior to deposition, the base pressure of $1x10^{-6}$ Torr was achieved inside the chamber. During deposition, the target and substrate distance of 5 cm was fixed inside the chamber. During sputtering process, the deposition pressure of $1x10^{-2}$ Torr (10 mTorr) was kept constant in Ar (50%) and N_2 (50%) gas ambient using mass flow controller. The thickness of the SiCN thin film was controlled with deposition time. Here, SiCN thin film was obtained at RF power of 150 W for 1.5 hr at room temperature. Finally, the SiCN/PSi sensing structure was decorated by Pd layer of thickness ~5 nm using dc sputtering for 5 s. Thereafter, for electrical characterization, the top silver conducting electrodes of 0.5 mm diameter were deposited via metal shadow mask using DC magnetron sputtering technique. Ag dots over the prepared thin film samples were synthesized at sputtering power and pressure of 30 W and 5 mT respectively for time period of 2 minutes using Ag target.

2.3 Characterization

To find the crystal structure, X-ray diffraction (XRD) patterns of SiCN thin film samples were performed by X-ray diffractometer with Cu K-α1 radiation of wavelength λ = 1.5406 Å in (θ -2θ) geometry (Co: Bruker AXS, D8 advance). Surface morphology and cross-sectional view analysis of all the synthesized thin film samples were examined at room temperature using field emission scanning electron microscopy (FE-SEM). The chemical state and elemental composition analysis of the as prepared thin film samples were studied using various spectroscopy techniques present in our laboratory such as Energy Dispersive Spectroscopy (EDS, attached with FE-SEM), and Raman spectroscopy. For electrical measurements, the silver paste was used to make the suitable electrical contacts over the SiCN thin film samples. A custom made sensing system having a volume of 300 cm^3. It consists a PID controlled electric heater for monitoring the live temperature of the chamber. A mass flow controller (MFC) is also attached with the sensing system for monitoring the desired ratio of inserted gases during sensing measurements. Figure 2 depicts the sketch of sensing setup used to measure the several gas sensing properties under different operating conditions. All the in situ sensing measurements were observed using two-probe resistivity method. In addition, the detailed analysis of output sensing characteristics was completed by origin software.

3. Result and discussion

3.1 Structural properties of sensing element

Figure 3a shows the XRD curve of Pd/SiCN thin film sample prepared on the porous silicon substrate. The XRD peak corresponds to the (311) plane was found at ~ 56.67 °. It confirms the cubic phase of silicon (JCPDS ICDD No. 00-001-0791). It can be seen that no XRD peak was found corresponds to SiCN, illustrating the amorphous nature of SiCN thin film.

Figure 3b depicts the transmission mode FTIR spectra of as-deposited SiCN thin films. FTIR spectra exhibit four absorption bands at ~ 434, 780, 960, and 1230 cm^{-1} respectively. The weak intensity bands found at ~434 and ~975 cm^{-1} resembles to asymmetric and symmetric stretching vibration of Si-N bond [30, 31]. The wide absorption band positioned at ~780 cm^{-1} is related to stretching vibration of Si-C bond [32]. The last weak band situated around ~1240 cm^{-1} was related to C-N bond [33]. Thus, the presence of Si-C, C-N and Si-N absorption bands endorse the evolution of SiCN phase. Raman spectrum as represented in Fig. 3c shows four characteristic peaks centered at ~454, 796, 1080, and 1543 cm^{-1} respectively. The sharp peak at ~454 cm^{-1} corresponds to Si-Si bond of amorphous silicon [34]. Second broad band centered at ~796 cm^{-1} is assigned to transverse optical phonon mode of Si-C bond [35]. The last two weak bands located at ~1080 $cm^{-1}$and ~1543 cm^{-1} are associated to Si-N bond and graphitic C-C bonds respectively [32, 34]. Hence above structural characterization authenticate that the active thin film layer is made up of SiCN and is available for hydrogen sensing measurements.

Figure 4a shows the top surface morphology of Porous-Si substrate observed by FE-SEM. It clearly revealed that pores of about 2 μm in diameter were synthesized homogeneously on the top surface of p-Si (100) wafers using electrochemical etching technique. Figure 4 (b-c) depicts the FE-SEM surface micrograph of as-prepared Pd/SiCN nanonanoballs (NBs) sensing layer at different magnifications. It is observed that the average diameter of SiCN nano-balls is ~ 900 nm. In addition, the inset of Fig. 4c shows that the silicon pores were filled with Pd decorated SiCN using RF sputtering method at room temperature. It can be seen that the width of top layer of active sensing material (Pd/SiCN) above the pores is around ~ 1.2 μm. Moreover, the depth of the prepared silicon pores was found to be ~ 6 μm. Figure 4d shows the elemental analysis of the active Pd/SiCN sensing layer. It depicts the energy (keV) on the x-axis and intensity on y-axis respectively. It can be seen that, the atomic % of Pd, Si, C, N and O elements in the as prepared thin film sample was found to be 2.10, 35.48, 31.87, 23.22 and 7.33 respectively. Here, 'O' element might be observed due to formation of thin (~ 10 nm) insulating layer of SiO_2 on the porous silicon substrate.

3.2 Sensing performance

In resistive based gas sensors, the observed change in electrical resistance (either increasing or decreasing) will predominantly be depends on the nature (oxidizing or reducing) of interacting gas molecules and the type (n-type or p-type) of semiconducting sensing layer [36]. The reducing nature of the target gas molecules behaves like donors, and hence reduces the resistance value of the n-type sensing materials and reverse is true for sensing layer of p-type. On the other hand, oxidizing nature of the target gas molecules behaves like acceptor, resulting to rise in electrical resistance of n-type sensing layer, and reverse is true for p-type sensing layer. Herein, after inserting the H_2 into the testing chamber, the resistance starts to decline which reveals the n-type behavior of the synthesized Pd/SiCN NBs sensor. Thus, for reducing gas molecules the sensor response value in percentage (%) can be estimated as per the given Eq. 3.

$$\text{Sensor Response } (\%) = \frac{Ra - Rg}{Ra} 100 \qquad (3)$$

In Eq. 3, R_a and R_g represent the observed resistance values in atmosphere of dry air and target gas respectively. As it is already documented that the slight change in resistance or sensor response is because of the corresponding interaction of target gas molecules over the testing sensor surface [37]. During the sensing measurements, the response time is elapsed time taken by the signal to accomplish 90% of its maximum stable level and the recovery time is the time required to attain the 90% change of the maximum constant signal in dry synthetic air.

Figure 5a shows the change in the value of sensor response of the proposed Pd/SiCN sensor to 50 ppm hydrogen mixed in dry synthetic air versus operating temperature within the range of 40–450°C. These results indicate that the response is continuously enhancing through the entire temperature regime (40–450°C). It is because of fast chemical reaction energy between the target gas and top surface atoms can

be observed at high working temperatures. Moreover, the elevated operating temperature can stimulate the contact reaction between target gas molecules and the oxygen species, resulting to noticeably improve the sensing response [38]. As depicted in Fig. 5b, the change in response was investigated at 400°C towards different concentrations (2-200 ppm) of hydrogen gas in the dry synthetic air. It can be observed that the detection limit (5 ppm) of hydrogen is quite considerable at high operating temperature (400°C). In addition, these results indicate that the enhancement in response with rising the concentration of target gas is significant thoroughly. This remarkable response behavior can be documented to the porous nature of substrate material and large active surface area of as deposited Pd/SiCN nanoballs sensor element [29, 39]. Initially, after exposure to analyte gas molecules mixed in dry air get adsorbed over the sensor surface. Thereafter, gas molecules will chemically react with surface atoms and start to desorbed when the exposure of analyte gas molecules is stopped. In this process, the proposed nanostructured materials may provide a usual path for the fast allocation of chemically activated sites and transferred mobile charge carriers. The resistive behavior of proposed Pd/SiCN NBs sensor element can be explored using current-voltage (I–V) measurements performed in the presence and absence of hydrogen (50 ppm) at an operating temperature of 400 ºC (Fig. 5c). Here, we have found that the sensor exhibits a rectifying behavior so that the electrical conductivity enhances. It might be due to enhancing the number of charge carriers (i.e. electrons) after

introducing the analyte gas molecules in dry air [40].

Figure 5d, depicts the response versus time curve to 50 ppm hydrogen gas at an optimum temperature of 400°C. It shows that the proposed sensor can exhibits fast response and recovery times of 22 seconds and 34 seconds respectively. It indicates that the large active surface area of Pd/SiCN nanoballs sensor may provide the presence of an enormous number of reaction sites on the top surface of active layer which can contribute for fast detection rate of H_2 gas molecules [41].

For the proposed sensor element, the characteristics curves of response and recovery time were also examined at different hydrogen concentrations from 2 ppm to 200 ppm (Fig. 6a). These result shows that the response time is falling and recovery time is improving with continuously rising the exposure limit of H_2 gas. It is recognized to the diffusion limited kinetics which may occur at relatively low concentrations of analyte gas molecules [42]. It can be seen due to dissimilar reaction rate at different concentration of target gas at the top surface of sensing layer. At high concentrations, the analyte gas molecules may react fast and the adsorption rate of the interacting gas molecules increases. So that the response time starts to decline with continuously increasing the concentration of hydrogen gas at ppm level. On that other hand, the recovery time of the sensing element continuously increase with the exposure to high concentration of hydrogen gas molecules. It may be documented that during desorption, at high concentrations the desorption rate of gas molecules become slow which can take more time to desorb and caused to enhance the recovery time continuously. Figure 6b displays the selectivity test towards several health hazardous gases like H_2, H_2S and CO at 50 ppm level at 400°C. It exhibits the enhanced sensor response (~60.2%) to H_2 gas with a feeble response value (< 15%) towards the other gases, indicating the Pd/SiCN NBs sensor element as very selective to 50 ppm H_2 gas at

400°C. Figure 6c shows the stability characteristic of the sensor towards 50 ppm hydrogen at 400°C. These result reveals that the sensor indicate almost constant (~ 6% change from initial) response signal for 80 days, illustrating the improbable stability of the Pd/SiCN NBs sensor element at 400°C. After 80 days, the small decline (~ 6%) in response can be accredited to the multiple heating of sensing element for long time operating at 400°C [39]. Here, the wide band gap and good thermal conductivity of SiCN may cause to synthesize the stable sensing element which can work even at high temperatures.
Figure 6d depicts the repeatability characteristics of the proposed sensor to 50 ppm H_2 in dry synthetic air at 400°C. It clearly exhibits that nearly constant (~ 5% change) sensor signal was recorded up to 10th cycles. This small change in response may be attributed to consistent heating of sensing element during the sensor testing at 400°C [29]. In this work, we have recommended the use of porous Si substrates as base material for the synthesis of active sensing layer to manipulate the growth and structure of SiCN which causes to enhance its available surface area for the interaction of target gas molecules [36, 41]. Therefore, the results indicate that porous Si substrates (as a template) can offer the long term reproducible as well as stabile curves towards 50 ppm level of hydrogen at 400°C. Thus, the proposed sensing structure may include the new practice to fabricate a sensor device which is capable to detect trace amount (few ppm) of H_2 in extreme environmental conditions.

3.4 Sensing mechanism

In general, the gas sensing mechanism of chemiresistive based gas sensors may be examined using well known surface depletion layer model [44]. During sensing measurements, for resistive gas sensors, the change in resistance takes place due to adsorption and desorption process of incoming gas molecules over top of sensor surface [44]. C.N.R. Rao et al. reported that during gas sensing tests, the various nitrogen vacancies presented in the sensing layer can act as the sorption sites for target gas molecules [45]. It is also reported that the oxygen can be significantly adsorbed at the right positions of nitrogen vacancies [46]. Thus, in this case the adsorption of oxygen at the site of nitrogen vacancies of SiCN thin film element may play a decisive role in varying its electrical resistance upon exposure to hydrogen gas molecules. Graphic interpretation of the H_2 sensing mechanism of SiCN NBs sensor is illustrated in Fig. 7.

In addition, the sensing mechanism of SiCN electrode material towards hydrogen gas involves two basic steps: Firstly, the as prepared sensing electrode is inserted inside the testing chamber and it is exposed to dry air to achieve the stable base line resistance. In this process, the oxygen molecules present in air can be adsorbed on top surface of sensing layer. These adsorbed oxygen molecules under chemisorption process capture the electrons from the conduction band of working electron, resulting to form various oxygen species (O^- and O^{2-}) at different working temperatures [47]. So that the carrier concentration of the sensing layer SiCN decreases which causes to formed a depletion layer at the sensor surface, as a result the initial resistance (R_a) of the working electrode enhances. These reactions can be represented as follows:

$$O_{2(gas)} \rightarrow 2O_{(ads)} \quad (4)$$

$$O_{(ads)} + e^-_{(from\ SiCN)} \rightarrow O^- \quad (5)$$

In second step, when Pd/SiCN active sensing layer is exposed to hydrogen gas using mass flow controller, then at the interacting surface a thin layer of Pd may offers the lower reaction energy to hydrogen gas molecules. Therefore, at the interface, the catalytic reaction of Pd instantly dissociate the hydrogen gas molecules into H atoms which is called spill over effect [47]. As a result, we observed a fast and stable response towards H_2 which causes to decline the response and recovery time [40]. Thereafter, these H atoms react with the chemisorbed oxygen species (O^- and O^{2-}), resulting to form the hydroxyl OH^- groups at the surface [43]. These OH^- groups can react again with other H atoms present inside the testing chamber to form H_2O molecules. In this process, the free electrons are liberated back to the CB of SiCN layer. As a result, after dissociation of H_2 gas molecules, the resistance (R_g) offered by the surface of the sensing layer starts to decline which causes to improve the sensing performance {Eq. (4)-(6)}. In this step, the whole said processes can be demonstrated with the help of following reactions occur on the sensor surface as given below:

$$H_{2(gas)} \rightarrow 2H_{(ads)} \quad (6)$$

$$H_{(ads)} + O^- \rightarrow OH^- \quad (7)$$

$$OH^-{}_{(ads)} + H_{(ads)} \rightarrow H_2O + e^-_{(to\ SiCN)} \quad (8)$$

Here, during exposure to the hydrogen gas molecules, the resistance changes with the time continuously and the corresponding sensor signal is noted. Due to long term exposure, hydrogen gas molecules get accumulated at the interface. As a result, the reaction rate between hydrogen gas molecules and sensor surface reduces continuously and hence the sensor signal becomes almost stable. Thereafter, we stop the flow of target gas and during the recovery process, a charge accumulation layer decreases, resulting to recover the original resistance of the sensor device in the absence of hydrogen gas molecules [41].

4. Conclusion

In this work, authors prepared porous silicon (P-Si) substrates using electrochemical anodization process. These P-Si substrates were used as a template to achieved the high surface area of active sensing element. Highly dense Pd decorated SiCN nanoballs were in situ synthesized on P-Si wafers under optimized conditions via radio frequency (RF) sputtering technique. The sensor performance of the proposed high surface area Pd/SiCN nanoballs based sensing element was found to be improved significantly. This work exhibited sensor response of 60.2% with fast response/recovery times of (22 s/34 s) towards 50 ppm H_2 at working temperature of 400°C. Moreover, the excellent stability (for 80 days) and reproducibility (over 10th cycles) were also observed to 50 ppm of hydrogen in dry air. Therefore, the porous silicon template used as a modified silicon substrate, that may offer a new understanding to propose and design a sensor device with its remarkable capabilities to detect hydrogen gas in extreme environment.

Declarations

Acknowledgements

We appreciate the experimental support provided by Indian Institute of Technology (IIT) Delhi and *CCS Haryana Agricultural University, His*ar, India.

Authorship contributions

Narendra Singh: Writing original draft, Methodology, Formal analysis, Figure preparation. **Hans Kumar Singh:** Formal analysis, software, Data curation, **Mamta Rawat:** Figure preparation, Visualization, Formal analysis, **Mukesh Kumar:** Software, Data curation, Investigation, **Vinay Kumar:** Resources, Visualization, Investigation, **Arvind Kumar:** Writing- review and editing, Conceptualization, Validation.

Funding

No funding was available for this work

Data availability

Data will be made available on request.

Declaration of Competing Interests

The authors declare that they have no known competing financial interests or personal relationships that could have appeared to influence the work reported in this paper.

References

1. J. Wang, Y. Kwak, I. Lee, S. Maeng, G. H. Kim, Highly responsive hydrogen gas sensing by partially reduced graphite oxide thin films at room temperature, Carbon, 50 (11), 4061-4067 (2012). https://doi.org/10.1016/j.carbon.2012.04.053
2. Z. Zhang, X. Zou, L. Xu, L. Liao, W. Liu, J. Ho, X. Xiao, C. Jianga and JinchaiLia, Hydrogen gas sensor based on metal oxide nanoparticles decorated graphene transistor, Nanoscale, 7 10078 (2015). https://doi.org/10.1039/C5NR01924A.
3. S. Zhou, M. Xiao, F. Liu, J. He, Y. Lin, Sub-10 parts per billion detection of hydrogen with floating gate transistors built on semiconducting carbon nanotube film, Carbon, 180, 41-47 (2021). https://doi.org/10.1016/j.carbon.2021.04.076
4. Peiyu Duan, Qiangling Duan, Qingkui Peng, et al, Design of ultra-sensitive gas sensor based on self-assembled Pd-SnO_2/rGO porous ternary nanocomposites for ppb-level hydrogen, Sens. Actuators B: Chem., 369, 132280, (2022). https://doi.org/10.1016/j.snb.2022.132280.
5. S. H. Kim, K. S. Yun, Room-temperature hydrogen gas sensor composed of palladium thin film deposited on $NiCo_2O_4$ nanoneedle forest, Sens. Actuators B, 376, 132958 (2023).

https://doi.org/10.1016/j.snb.2022.132958

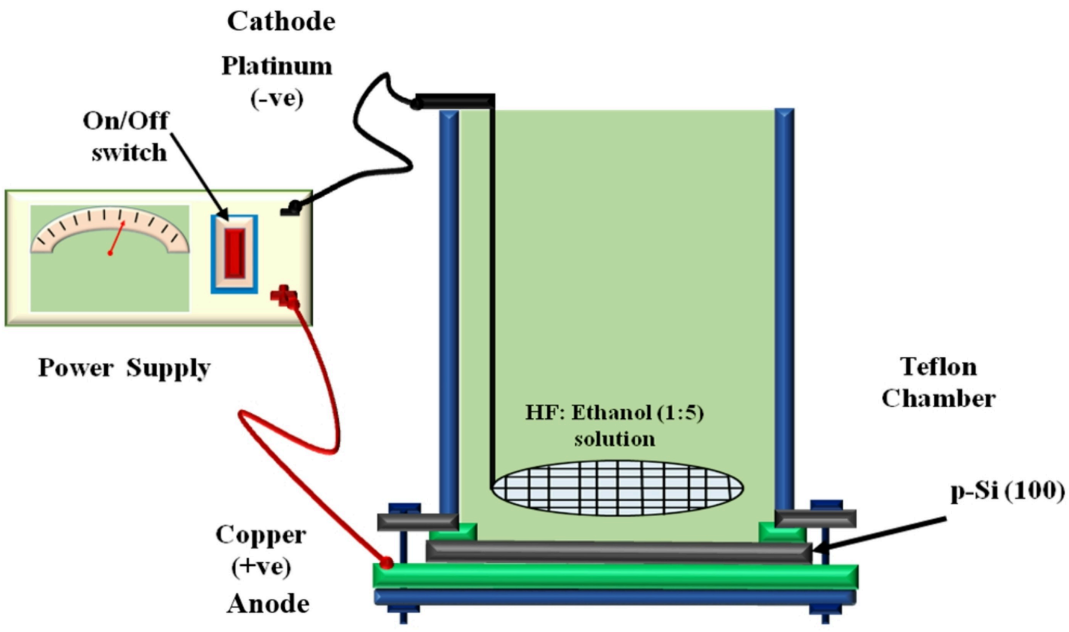
6. N. Kostoglou, C.W. Liao, C. Y. Wang, J. N. Kondo, C. Tampaxi, T. Steriotis, K. Giannakopoulos, A. G. Kontos, S. Hinder, M. Bake, E. Bousser, Effect of Pt nanoparticle decoration on the H_2 storage performance of plasma-derived nanoporous graphene, Carbon 171, 294-305 (2021). https://doi.org/10.1016/j.carbon.2020.08.061
7. B. Alfano, E. Massera, T. Polichetti, M. L. Miglietta, Effect of palladium nanoparticle functionalization on the hydrogen gas sensing of graphene based chemi-resistive devices, Sens. Actuators B: Chem., 253, 1163–1169 (2017). https://doi.org/10.1016/j.snb.2017.07.146
8. M. Kumar, V. S. Bhati, M. Kumar, Effect of Schottky barrier height on hydrogen gas sensitivity of metal/TiO_2 nanoplates, Int. J. Hydro. Energy, 42, 22082-22089 (2017). https://doi.org/10.1016/j.ijhydene.2017.07.144
9. J. G.Aguilar, I. M. García, Á. B. Murcia, D. C.Amorós, Single wall carbon nanotubes loaded with Pd and NiPd nanoparticles for H_2 sensing at room temperature, Carbon, 66, 599-611 (2014). https://doi.org/10.1016/j.carbon.2013.09.047
10. Liu, L., Guo, C., Wang, Y. *et al.* A comprehensive review of hydrogen sensor for thermal runaway monitoring: fundamentals, recent advancements, and challenges. *Microsyst Nanoeng* 12, 108 (2026). https://doi.org/10.1038/s41378-026-01171-x
11. A. Kumar, A. Sanger, A. Kumar and R. Chandra, Highly sensitive and selective CO gas sensor based on a hydrophobic SnO_2/CuO bilayer, RSC Adv. 6, 47178, (2016). https://doi.org/10.1039/C6RA06538D
12. Khnykov, A.Y., Vdovichenko, A.Y. Nanostructured Materials for Gas Sensors. *Nanotechnol Russia* 20, 101–117 (2025). https://doi.org/10.1134/S2635167625600051
13. A. Kaniyoor, S. Ramaprabhu, Hybrid carbon nanostructured ensembles as chemiresistive hydrogen gas sensors, Carbon, 49, 227 (2011). https://doi.org/10.1016/j.carbon.2010.09.008
14. F. Yun, S. Chevtchenko, Y. T. Moon, H. M. Timothy, J. Fawcett, GaN resistive hydrogen gas sensor, Appl. Phys. Lett. 87 (2005) 073507. https://doi.org/10.1063/1.2031930
15. S. Roy, C. Jacob, S. Basu, Studies on Pd/3C-SiC Schottky junction hydrogen sensors at high temperature, Sens. Actuators B: Chem., 94 (2003) 298–303. https://doi.org/10.1016/S0925-4005(03)00380-0
16. Kim, C.K., Lee, J.H., Lee, Y.H. *et al.* Hydrogen sensing characteristics of Pd-SiC schottky diode operating at high temperature. *J. Electron. Mater.* 28, 202–205 (1999). https://doi.org/10.1007/s11664-999-0014-1.
17. G. Miiller and G. Krotz, E. Niemann, SiC for sensors and high-temperature electronics, Sensors and Actuators A: Physical, 43 259-268 (1994). https://doi.org/10.1016/0924-4247(93)00684-V
18. Kumar, Y.N.S., Asri, R.I.M., Ramzan, M. *et al.* Advances in fabrication techniques for porous GaN: a review of methods and applications. *J Mater Sci: Mater Electron* 36, 1774 (2025). https://doi.org/10.1007/s10854-025-15728-5.

19. M. T. Sooa, K. Y. Cheonga, A. F. Noor, Advances of SiC-based MOS capacitor hydrogen sensors for harsh environment applications, Sens. Actuators B: Chem.,151, 39–55, (2010). https://doi.org/10.1016/j.snb.2010.09.059.
20. Jianjun Chen, Judong Zhang, Mingming Wang, Ye Li, High-temperature hydrogen sensor based on platinum nanoparticle-decorated SiC nanowire device, Sens. Actuators B: Chem., 201, 401-406 (2014). https://doi.org/10.1016/j.snb. 2014.04.068
21. A. Trinchi, S. Kandasamy, W. Wlodarski, High temperature field effect hydrogen and hydrocarbon gas sensors based on SiC MOS devices, Sens. Actuators B: Chem., 133 705–716 (2008). https://doi.org/10.1016/j.snb.2008.03.011.
22. Mun Teng Soo, Kuan Yew Cheong, Ahmad Fauzi Mohd Noor, Advances of SiC-based MOS capacitor hydrogen sensors for harsh environment applications, Sens. Actuators B: Chem., 151, 39-55 (2010). https://doi.org/10.1016/j.snb.2010.09.059.
23. C. K. Kim, J. H. Lee, S. M. I. H. Noh, Choi, H. R. Kim, N. I. Cho, C. Hong, G. E. jang, Pd- and Pt-SiC Schottky diodes for detection of H_2 and CH_4 at high temperature, Sens. Actuators B: Chem., 77, 455-462 (2001). https://doi.org/10.1016/S0925-4005(01)00725-0.
24. E. Tomasella, F. Rebib, M. Dobois, J. Cellier, and M. Jacquet, Structural and optical properties studies of sputtered a-SiCN thin films, J. Phys. Conf. Ser.100, 082045 (2008). https://doi.org/10.1016/j.apsusc.2010.11.166.
25. Tran, K.N., Tran, H.N.Q., Abell, A.D. *et al.* Nanoporous anodic alumina-based gas sensors: insights into advances and perspectives. *Microchim Acta* 192, 441 (2025). https://doi.org/10.1007/s00604-025-07234-6.
26. J. H. Lee, Gas sensors using hierarchical and hollow oxide nanostructures: Overview, Sens. Actuators B, 140 (2009) 319–336.
27. Y. Zhang, J. Xu, Qun Xiang, Hui Li, Qingyi Pan, and Pengcheng Xu, Brush-Like Hierarchical ZnO Nanostructures: Synthesis, Photoluminescence and Gas Sensor Properties, J. Phys. Chem. C 113 (2009) 3430–3435.
28. Mutar, Z.S., Mutlak, F.AH. The Role of Illumination on Electrochemically Etched Silicon Nanostructures for Gas Sensing Applications. *Silicon* 18, 1247–1265 (2026). https://doi.org/10.1007/s12633-025-03615-x
29. A. Kumar, A. Kumar, Ramesh Chandra, Fabrication of porous silicon filled Pd/SiC nanostructured thin films for high performance H_2 gas sensor. Sens. Actuators B, 264 (2018) 10-19. https://doi.org/10.1016/j.snb.2018.02.164.
30. X. Peng, L. Song, J. Meng, Y. Zhang, X. Hu, Preparation of silicon carbide nitride thin films by sputtering of silicon nitride target, Appl. Surf. Sci 173 (2001) 313-317. https://doi.org/10.1016/S0169-4332(01)00010-1.
31. W. F. A. Besling, A. Goossens, B. Meester, and J. Schoonman, Laser-induced chemical vapor deposition of nanostructured silicon carbonitride thin films, J. Appl. Phys., 83, 544 (1998). https://doi.org/10.1063/1.366669.

32. Y. Gao, U, J. Wei, D.H. Zhang, Z. Q. Mo, P. Hing, X. Shi, Effects of nitrogen fraction on the structure of amorphous silicon carbon nitrogen alloys, Thin Solid Films, 378, 562-566 (2000). https://doi.org/10.1016/s0040-6090(00)01292-x.
33. P. Gao, J. Xu, Y. Piao, W. Ding, D. Wang, X. Deng, C. Dong, Deposition of silicon carbon nitride thin films by microwave ECR plasma enhanced unbalance magnetron sputtering, Surf. Coat. Techn. 201, 5298-5301 (2007). https://doi.org/10.1016/j.surfcoat.2006.07.197.
34. X. Xiao, Y. Li, L. Song, X. Peng, X. Hu, Structural analysis and microstructural observation of SiCN films prepared by reactive sputtering of SiC in N_2 and Ar, Appl. Surf. Sci. 156, 155-160 (2000). https://doi.org/10.1016/s0169-4332(99)00493-6.
35. N. M. Park, S. H. Kim, and G. Y. Sung, Band gap engineering of SiCN film grown by pulsed laser deposition, J. Appl. Phys. 94, 2725 (2003). https://doi.org/10.1063/1.1594267.
36. K. S. Kim, G. S. Chung, Characterization of porous cubic silicon carbide deposited with Pd and Pt nanoparticles as a hydrogen sensor, Sens. Actuators B: Chem., 157, 482 (2011). https://doi.org/10.1016/j.snb.2011.05.004.
37. A. Sanger, A. Kumar, A. Kumar, J. Jaiswal, R. Chandra, A fast response/recovery of hydrophobic Pd/V_2O_5 thin films for hydrogen gas sensing, Sens. Actuators B: Chem., 236, 16-26 (2016). https://doi.org/10.1016/j.snb.2016.05.141.
38. A. Kumar, A. Sanger, A. Kumar, R. Chandra, Porous silicon filled with Pd/WO_3-ZnO composite thin film for enhanced H_2 gas-sensing performance, RSC Adv., 7, 39666 (2017). https://doi.org/10.1016/j.snb.2016.04.152.
39. J. Chen, J. Zhang, M. Wang, Y. Li, High-temperature hydrogen sensor based on platinum nanoparticle-decorated SiC nanowire device, Sens. Actuators B: Chem., 201 (2014) 402-6. https://doi.org/10.1016/j.snb.2014.04.068.
40. A. Sanger, A. Kumar, A. Kumar, R. Chandra, Highly sensitive and selective hydrogen gas sensor using sputtered grown Pd decorated MnO_2 nanowalls, Sens. Actuators B: Chem., 234 8-14 (2016). https://doi.org/10.1016/j.snb.2016.04.152
41. K. S. Kim, G. S. Chung, Fast response hydrogen sensors based on palladium and platinum/porous 3C-SiC Schottky diodes, Sens. Actuators B: Chem., 160, 1232 (2011). https://doi.org/10.1016/j.snb.2011.09.054.
42. S. J. Choi, S. Chattopadhyay, J. J. Kim, S. J. Kim, H. L. Tuller, G. C. Rutledge, et al., Coaxial electrospinning of WO_3 nanotubes functionalized with bio-inspired Pd catalysts and their superior hydrogen sensing performance, Nanoscale, 8, 9159-9166 (2016). https://doi.org/10.1039/c5nr06611e.
43. Q. Qi, T. Zhang, X. Zheng, H. Fan, L. Liu, R. Wang, Electrical response of Sm_2O_3-doped SnO_2 to C_2H_2 and effect of humidity interference, Sens. Actuators B: Chem, 134, 36-42 (2008). https://doi.org/10.1016/j.snb.2008.04.011.

44. J. Guo, J. Zhang, M. Zhu, D. Ju, H. Xu, B. Cao, High-performance gas sensor based on ZnO nanowires functionalized by Au nanoparticles, Sens. Actuators B: Chem., 199 339-345 (2014). https://doi.org/10.1016/j.snb.2014.04.010
45. B. Chitara, D. J. Late, S. B. Krupanidhi, C.N.R. Rao, Room-temperature gas sensors based on gallium nitride nanoparticles, Solid State Communication, 150, 2053-2056 (2010). https://doi.org/10.1016/j.ssc.2010.08.007.
46. D. S. Lee, J. H. Lee, Y. H. Lee, D. D. Lee, GaN thin films as gas sensors, Sens. Actuators B: Chem. 89, 305-310 (2003). https://doi.org/10.1016/s0925-4005(03)00008-x.
47. Q. N. Abdullah, F. K. Yam, Z. Hassan, M. Bououdina, Hydrogen gas sensing performance of GaN nanowires-based sensor at low operating temperature, Sens. Actuators B: Chem., 204 497-506 (2014). https://doi.org/10.1016/j.snb.2014.07.112.

Figures



Schematic view of the fabrication process of porous silicon using electrochemical anodization.

Figure 1

Schematic for the preparation of porous silicon (PS) substrates using electrochemical anodization method.

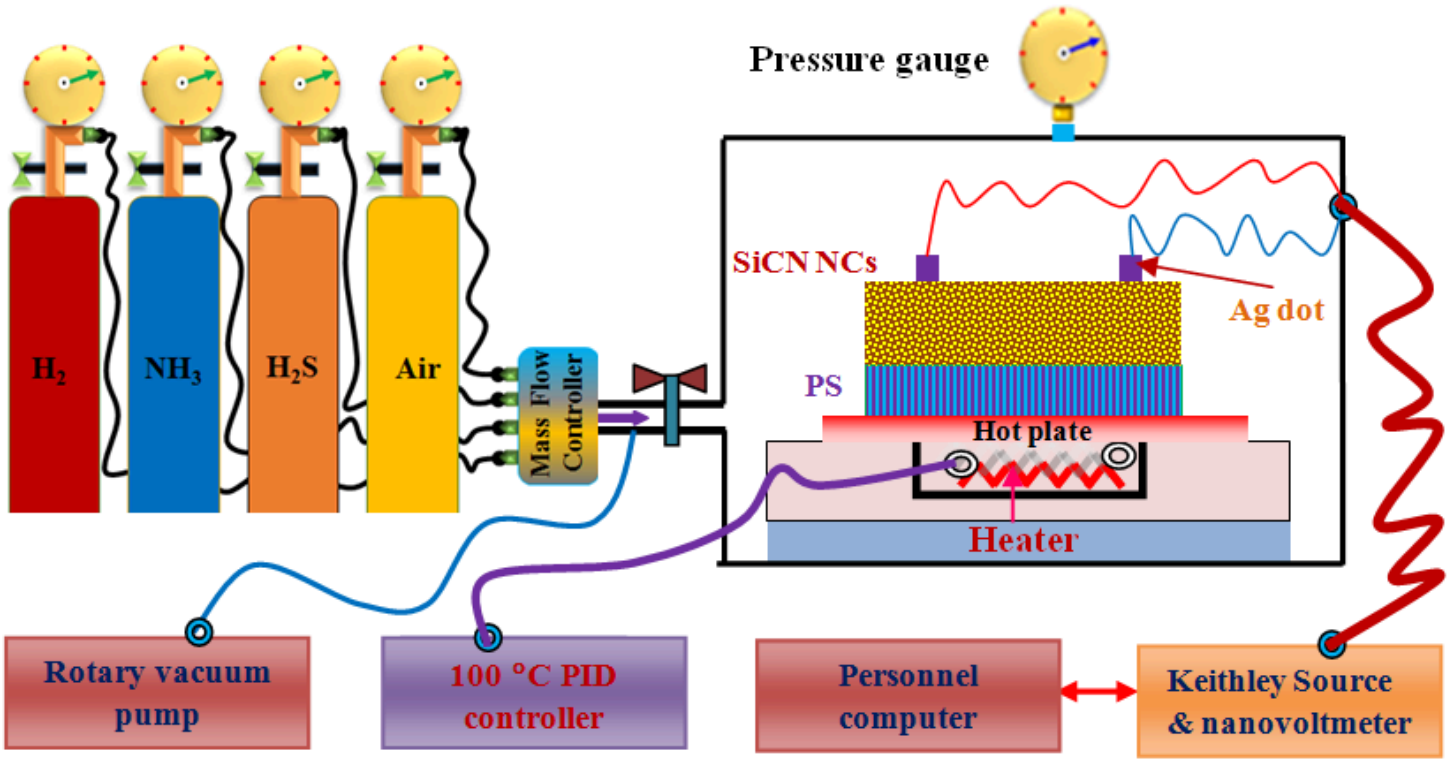


Figure 2

Schematic diagram of the sensing measurement setup.

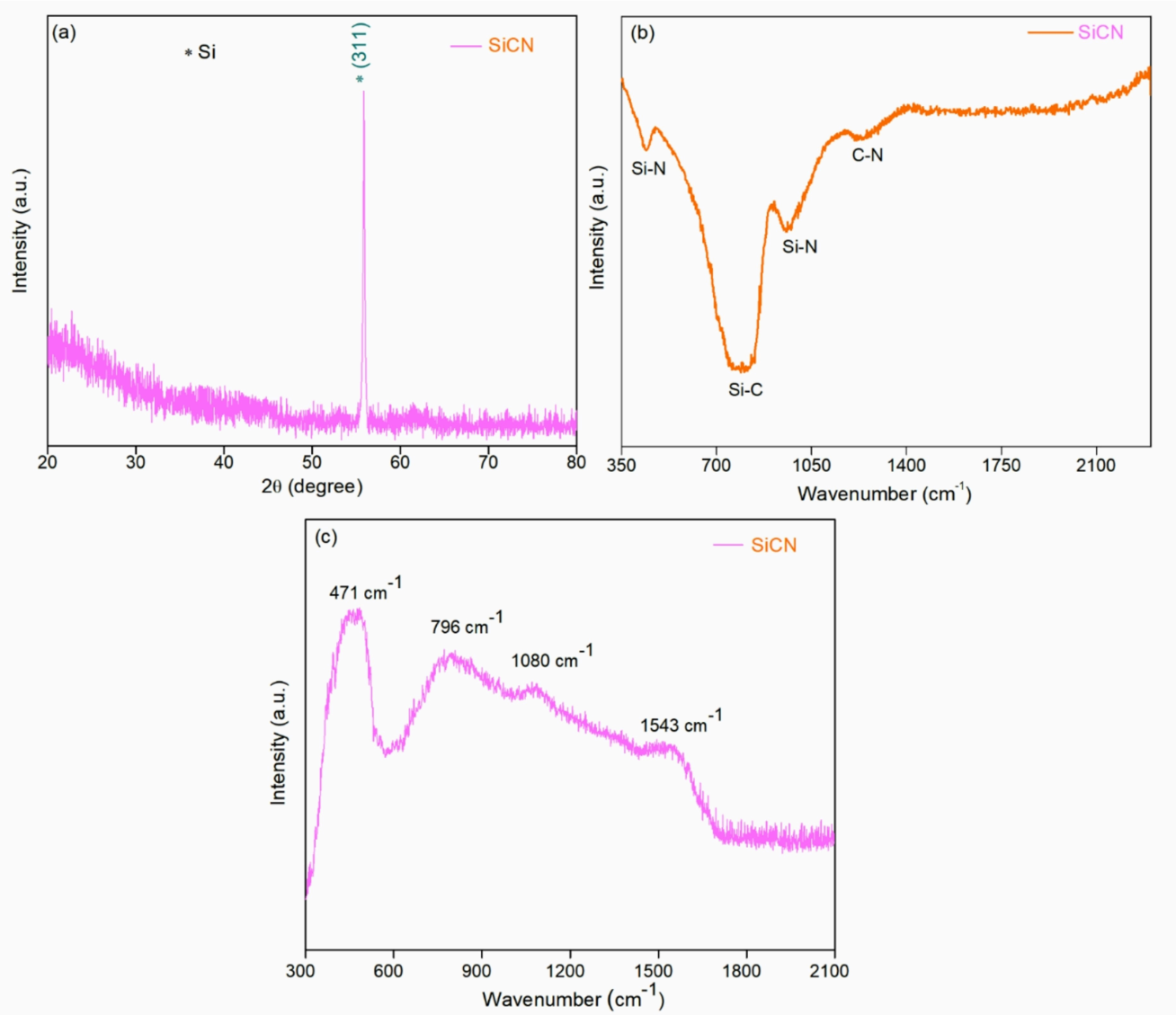


Figure 3

(a) Room temperature XRD curve, (b) FTIR spectra (c) Raman spectra of SiCN sensing electrode material.

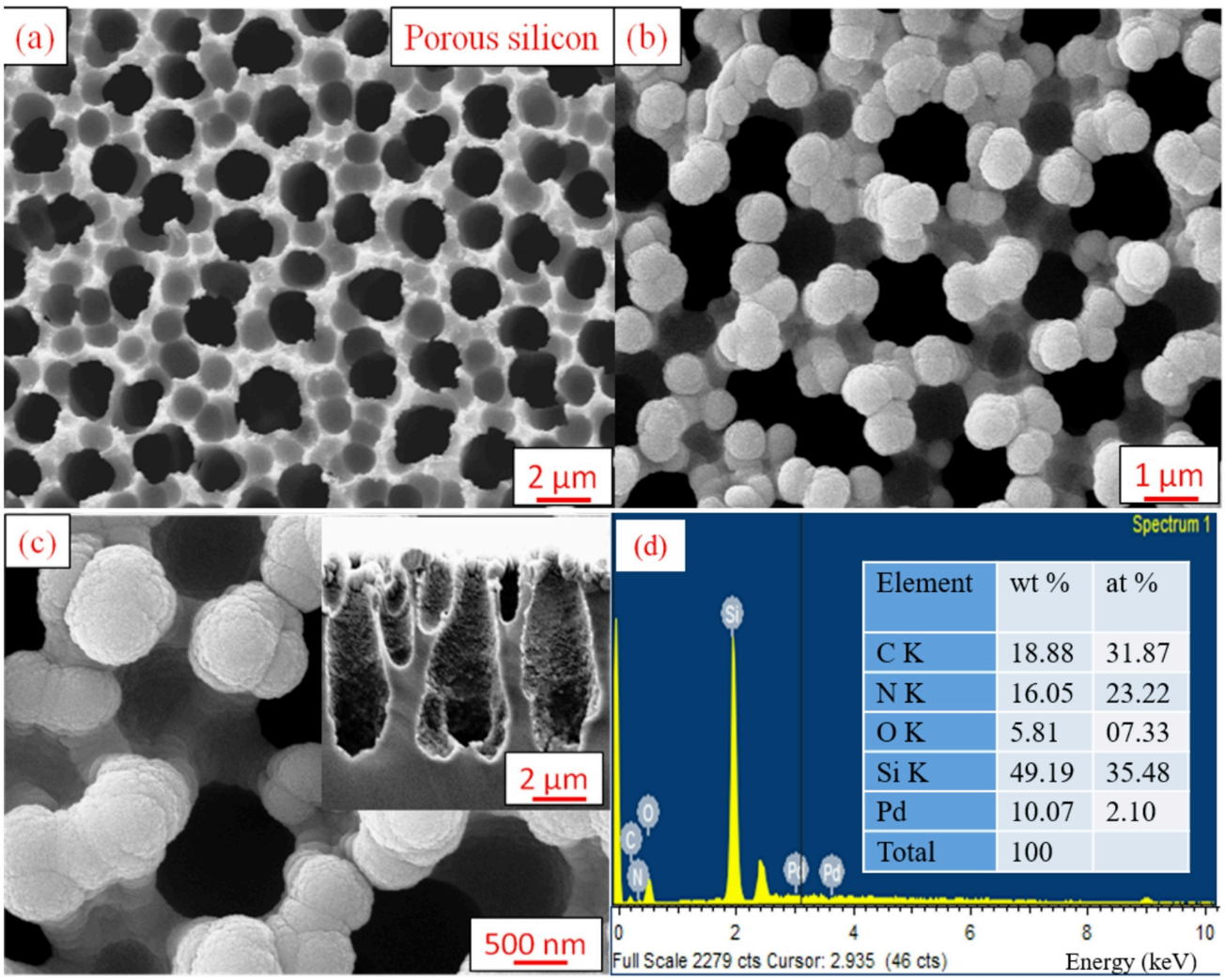


Figure 4

(a) FE-SEM surface micrograph of the porous silicon (PS) substrate, (b)-(c) FE-SEM surface morphology of Pd-capped SiCN sensing layer at low and high magnification respectively, inset of (c) is the cross-sectional FESEM image and (d) EDS analysis of the Pd/SiCN thin film sample.

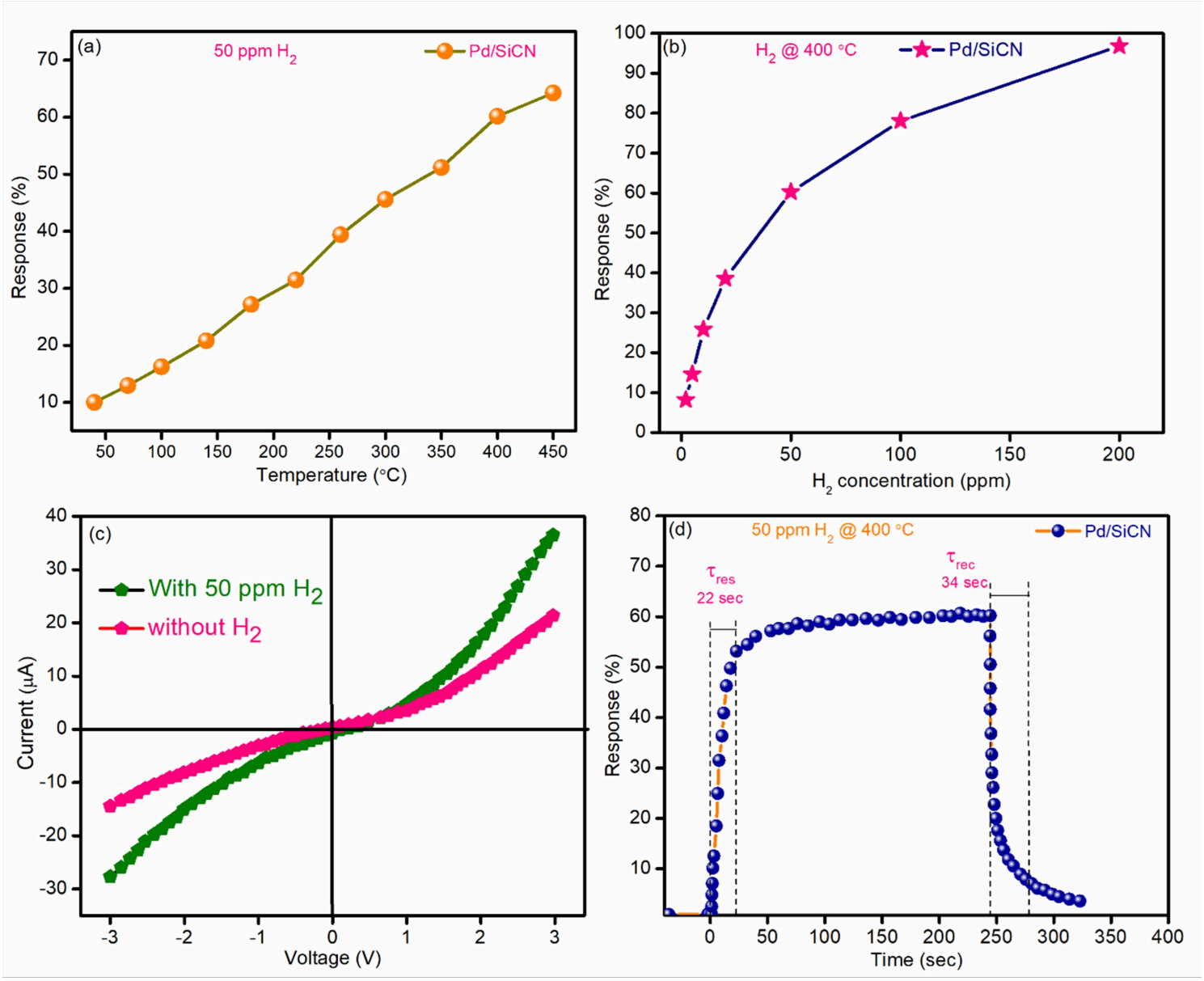


Figure 5

(a) Gas response curve vs. operating temperature for 50 ppm hydrogen gas, (b) variation of response with hydrogen gas concentration (2-200 ppm) at 400 °C, (c) current-voltage (I-V) characteristics curve of Pd/SiCN nanoball sensor at 400 °C, (d) gas response versus time curve for 50 ppm hydrogen gas at operating temperature of 400 °C.

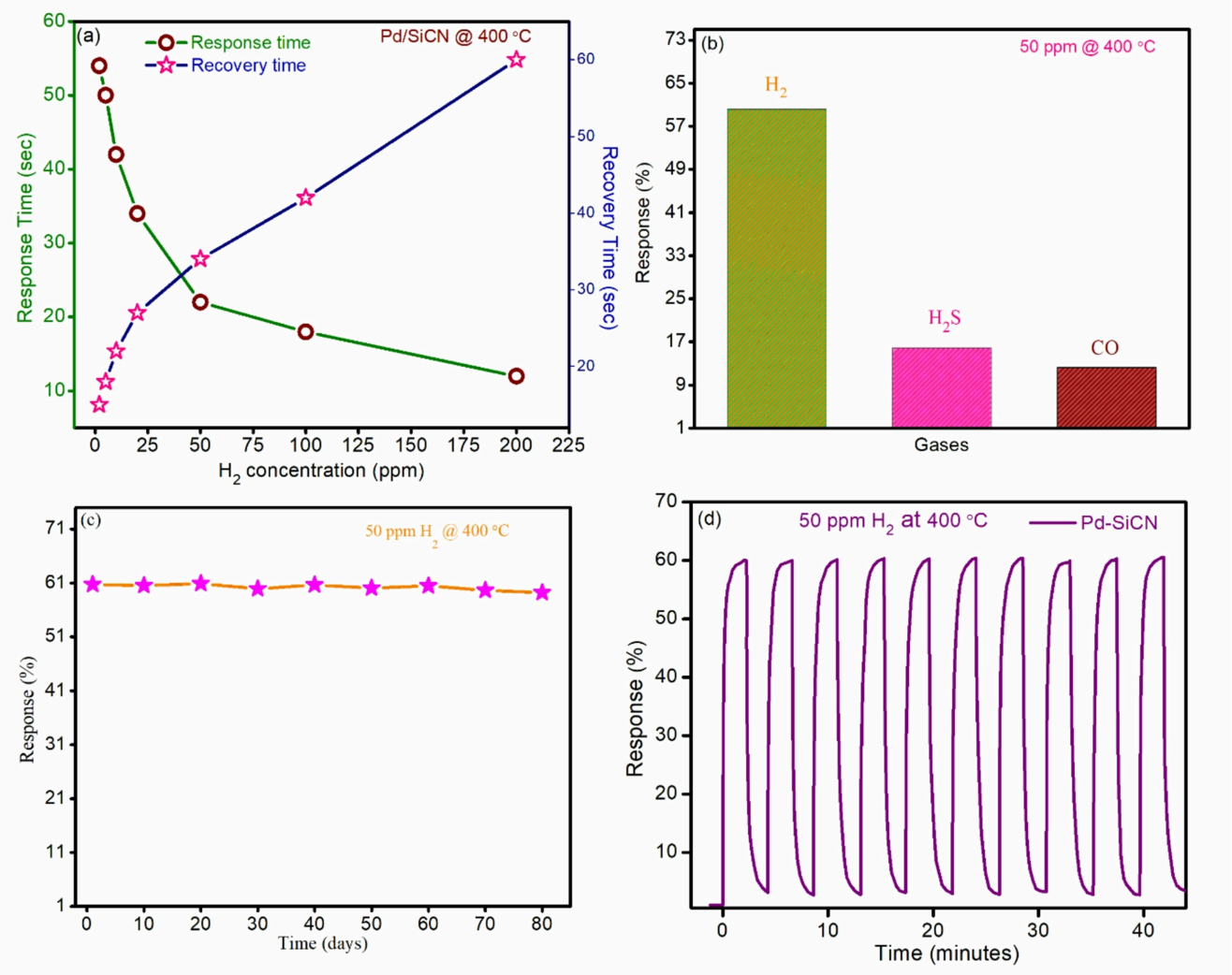


Figure 6

(a) Response and recovery time curve vs. hydrogen gas concentration (2-200 ppm) at 400 °C for Pd/SiCN nanoball sensor, (b) cross selectivity test of Pd-capped SiCN nanoballs sensor at 50 ppm level at high operating temperature of 400 °C, (c) response time behavior of the proposed device for 80 days, indicating long term stability of the sensor at 400 °C, (d) the cyclability measurements of Pd/SiCN nanoballs sensor up to 10^{th} cycles at 400 °C.

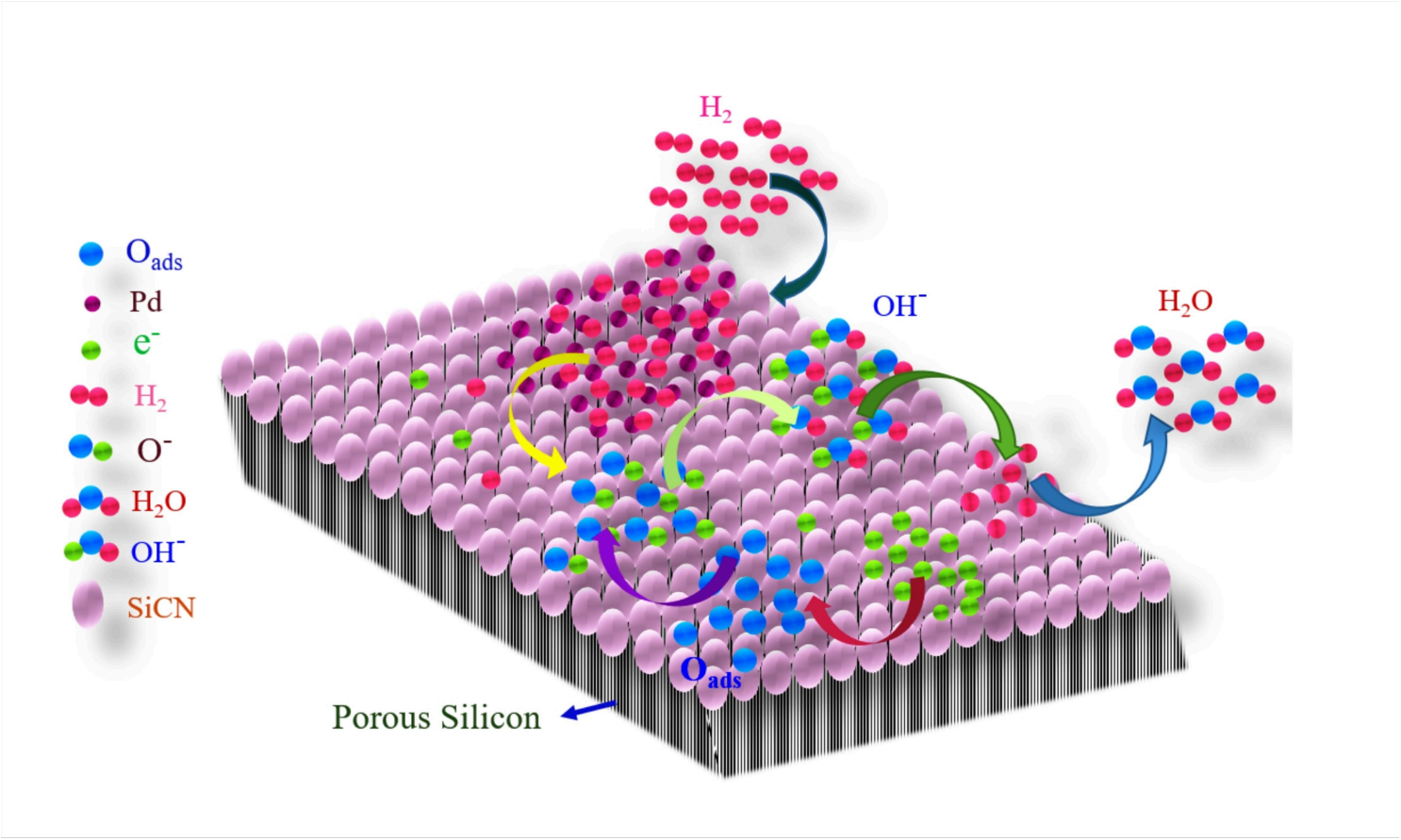


Figure 7

Schematic illustration of hydrogen gas sensing mechanism of Pd decorated SiCN nanoballs